



Published in final edited form as:

Placenta. 2020 April ; 93: 1–7. doi:10.1016/j.placenta.2020.02.006.

## Nanoparticle mediated increased *insulin-like growth factor 1* expression enhances human placenta syncytium function

Rebecca L. WILSON, Ph.D<sup>1,\*</sup>, Kathryn OWENS, B.Sc<sup>1</sup>, Emily K. SUMSER<sup>1</sup>, Matthew V. FRY, B.S<sup>1</sup>, Kendal K. STEPHENS, M.D<sup>1</sup>, Marcel CHUECOS, BS<sup>2</sup>, Maira CARRILLO, PhD<sup>2</sup>, Natalia Schlabritz-Loutsevitch, M.D. Ph.D<sup>2</sup>, Helen N. JONES, Ph.D<sup>1</sup>

<sup>1</sup>Center for Fetal and Placental Research, Cincinnati Children's Hospital and Medical Center, Cincinnati, Ohio, USA 45229.

<sup>2</sup>Texas Tech University Health Sciences Center at the Permian Basin, Odessa, TX, USA, 79763

### Abstract

**Introduction:** Placental dysfunction is an underlying cause of many major obstetric diseases and treatment options for complications like fetal growth restriction (FGR) are limited. We previously demonstrated nanoparticle delivery of the *human insulin-like growth factor 1 (hIGF1)* transgene under control of the trophoblast-specific PLAC1 promoter maintains normal fetal growth in a surgically-induced FGR mouse model. However, uptake by human placental syncytiotrophoblast has yet to be determined.

**Methods:** An *ex vivo* human placenta perfusion model, term placenta villous fragments and other *in vitro* syncytiotrophoblast models, were used to determine nanoparticle uptake, transgene expression and functional responses under oxidative stress conditions.

**Results:** In the *ex vivo* perfusion, fluorescence from a Texas-Red conjugated nanoparticle increased in maternal perfusate upon nanoparticle addition and declined by the conclusion of the experiment ( $P < 0.001$ ). Fluorescent histology confirmed localization in the syncytiotrophoblasts. No Texas-Red fluorescence was detected in the fetal perfusate. Transgene expression of *hIGF1* in differentiated BeWo cells, isolated primary trophoblasts and fragments was increased compared to untreated (55,000-fold,  $P = 0.0003$ ; 95-fold,  $P = 0.003$ ; 400-fold,  $P < 0.001$ , respectively). Functionally, increased *hIGF1* expression in villous fragments resulted in translocation of glucose transporter 1 to the syncytiotrophoblast cell membrane and under conditions of oxidative stress in BeWo cells, protected against increased cell death ( $P < 0.01$ ) and decreased mitochondrial activity ( $P < 0.01$ ).

\*Corresponding Author: Rebecca Wilson, CFPR, Cincinnati Children's Hospital and Medical Center, 3333 Burnet Ave, Cincinnati OH 45229, Phone: 513 803 4338, Rebecca.Wilson@cchmc.org.

**Author contributions:** RLW contributed substantially to experimental design, performed experiments, analyzed data, and wrote and revised the manuscript. KO contributed significantly to data acquisition and analysis. EKS contributed significantly to experimental design and data acquisition. MF contributed significantly to data acquisition and analysis. KKS contributed significantly to data acquisition. NS-L, MCh and MCa contributed significantly to experimental design and data acquisition and analysis. HNJ contributed significantly to concept and study design, data acquisition, analysis and interpretation. All authors have contributed to drafting the manuscript and have approved the final submitted version.

**Publisher's Disclaimer:** This is a PDF file of an unedited manuscript that has been accepted for publication. As a service to our customers we are providing this early version of the manuscript. The manuscript will undergo copyediting, typesetting, and review of the resulting proof before it is published in its final form. Please note that during the production process errors may be discovered which could affect the content, and all legal disclaimers that apply to the journal pertain.

**Conclusion:** The current study confirms that our nanoparticle is capable of uptake in human placental syncytium which results in enhanced transgene expression, functional changes to cellular activity and protection against increased oxidative stress.

### Keywords

Placenta; Nanoparticle; Insulin-Like Growth Factor; Fetal Growth Restriction; Pregnancy; Therapy; Placental Dysfunction

---

### Introduction

Most major pregnancy complications including preeclampsia (high blood pressure and widespread systemic endothelial dysfunction), stillbirth and fetal growth restriction are characterized by aberrant placental development and function. Such complications predict significant morbidity and mortality for both mother and child and treatment options *in utero* are limited [1]. The placenta is the interface involved in the exchange of gases, nutrients and wastes between the mother and fetus and is vital to the growth of the fetus. Maternal and fetal circulation within the placenta remains separated and thus the transfer of nutrients, oxygen, and waste occurs across several layers of cells [2]. Cells making up the outer most layer that are in contact with maternal blood are the syncytiotrophoblasts; a multinucleated syncytium formed by fusion of the underlying cytotrophoblasts [3]. Absence of lateral cell boundaries and intercellular junctions indicates that molecules need to be exchanged across the apical and basal membranes of the syncytiotrophoblast [2] and thus represents a challenge when developing therapies that target the placenta.

Our laboratory has developed a non-viral transgene delivery method of human insulin-like growth factor 1 (*hIGF1*) in the form of a biodegradable nanoparticle that results in trophoblast-specific expression of *hIGF1*. IGF1 is important for fetoplacental development and has been shown to regulate metabolic effects, mitogenesis, differentiation, and survival in various organs including the placenta [4]. *Igf1* null mice are 60% lighter in body weight compared to wild-type littermates and have a 95% perinatal morbidity rate highlighting the significance of IGF1 in fetal growth and development [5]. Clinically, a reduction in IGF1 concentration in fetal cord sera is associated with intra-uterine growth restricted (IUGR) or small for gestational age (SGA) newborns [6, 7]. We have shown that intra-placental injections of the nanoparticle containing *hIGF1* results in overexpression of *hIGF1* in a murine model of placental insufficiency and maintenance of normal fetal growth [8]. Additionally, overexpression of *hIGF1* in the human choriocarcinoma BeWo cell line, a model of human cytotrophoblasts, results in increased cell proliferation, reduced apoptosis, and increased expression of System A and L amino acid transporters [9].

In order to continue establishing translational potential, we aimed to determine if the nanoparticle could be taken up by the human placental syncytium using a short-term dual placental perfusion model *ex vivo*. Furthermore, we assessed *hIGF1* expression in 3 *in vitro* models that mimic the syncytial properties of the human placenta and characterized the functional response of placental cells to oxidative stress when treated with nanoparticle.

## Materials and Methods

### Nanoparticle formation

The *PLAC1-hIGF1* plasmid was cloned as previously described [8] and purified using an Endo-Free Plasmid Maxi Kit (*Qiagen*) as per manufacturer's instructions. The yield, purity, and integrity of the plasmids were assessed with a Nanodrop® (*Thermo Scientific*). To create the nanoparticles, lyophilized poly-(HPMA)<sub>115</sub>-b-poly(DMAEMA)<sub>115</sub> copolymer was reconstituted in ultra-pure water and incubated with 1 µg of plasmid at a DNA (µg):polymer (µL) ratio of 1:4 (BeWo and isolated cytotrophoblast experiments) or 1:10 (placenta fragment experiments) in calcium and magnesium free phosphate buffered saline (PBS) for 1 h at room temperature prior to use. BeWo and isolated cytotrophoblast cells were treated with 8 µg of DNA/well; placental fragment were treated with 33 µg of DNA/well.

For the *ex vivo* placenta perfusion experiments, the HPMA<sub>110</sub>-DMAEMA<sub>33</sub> copolymer was conjugated with a Texas Red fluorophore in order to trace movement of the nanoparticle into the placenta tissue. Texas Red™-X, succinimidyl ester (5 mg; *Invitrogen*) was modified by incubating for 24 h at 30°C in a solution of dimethylformamide (DMF) and ethylene diamine. After the solvent was removed, the product was purified by flash column chromatography. Conjugation occurred by incubating the modified Texas-Red product in a solution containing the HPMA<sub>110</sub>-DMAEMA<sub>33</sub> copolymer at 30°C for 48 h, dialyzing against distilled water for 3 days and lyophilizing. Following reconstitution, the Texas-red conjugated copolymer was incubated with 1 µg plasmid at a ratio of 1:20 DNA to polymer.

### Ex vivo dual human placenta perfusion

Placentas (n=7: 5 females and 2 males) at term ( 39 weeks gestation) of appropriate birthweight and without any diagnosed pregnancy complications were obtained elective Caesarian sections (due to previous Caesarian deliveries) at the according to the protocol, published elsewhere [10]. Placental perfusion protocol was approved by TTUHSC IRB (#L15-108). Dual perfusion was performed as previously described [11]. Total experimental duration ranged from 3.5–4.5 h with the initial open system duration lasting 1.5–2 h followed by a closed system duration of 0.5–1.5 h before Texas-red conjugated nanoparticle were added to perfusate on the maternal side for approximately 1 h. Fetal hydrostatic inflow pressure (FIP) was measured constantly during experiments and feto-maternal leakage was measured every 0.5 h using estimated FITC-conjugated dextran, which were paralleled by the measurements of the outflow using a glass 10 mL graduated measuring cylinder. Barrier function throughout the perfusion was assessed by analyzing glucose uptake, lactate production and oxygen uptake. Of the 7 placentas perfused, only one did not pass quality assurance; no nanoparticle was added to the maternal perfusate, and therefore served as a negative control for histological analysis. Maternal and fetal venous perfusate samples were obtained prior to addition of the nanoparticle, at nanoparticle addition and at conclusion of the experiment; recovery rate of the perfusate was 100%. Placenta tissue samples were also collected, fixed in 10% formalin and frozen in OCT for histological analysis. One placenta, in which nanoparticle was not added, served as a negative control. Fluorescence of the perfusate samples was quantified at 625 nm in triplicate using a micro-titre plate reader

(Synergy H1 Hybrid; *Biotek*). Histological analysis of nanoparticle localization was determined in 7  $\mu\text{m}$  tissue sections visualized using the Nikon Eclipse Ti Inverted microscope. Quantification was performed using ImageJ Image analysis software by limiting a threshold to the Texas-red fluorescence and calculating integrated density of the threshold only.

### Tissue collection for in vitro studies

For human isolated cytotrophoblasts (n=4) and fragment experiments (n=6), term ( 39 weeks gestation) placentas from pregnancies in which maternal age was <45 years, BMI was between 18–30  $\text{kg}/\text{m}^2$  and delivered an appropriate for gestational age infant with no diagnosis of any maternal or fetal complications were collected following Caesarean section or vaginal delivery under the approval of Good Samaritan Hospital and Cincinnati Children’s Hospital Medical Center Institutional Review Boards. Tissue was transferred to the laboratory within 45 mins of delivery and processed as outlined below.

### Differentiated BeWo and isolated cytotrophoblast cell culture

Human BeWo choriocarcinoma cells (CCL-98; *American Type Culture Collection*) were cultured and treated in HAM’s F12 nutrient mix supplemented with 10% fetal bovine serum (FBS) and 1% penicillin/streptomycin and maintained at 37° C under 5% CO<sub>2</sub>. All cells were between passages 4 and 12.  $1 \times 10^5$  BeWo cells/well were seeded onto 6-well plates and incubated with 50  $\mu\text{M}$  forskolin (FK) in DMSO (*EMD Millipore*) or DMSO only (controls) for 48 h, changing the media at 24 hours. Cells were then allocated to one of 4 treatment groups: untreated (*Control*), FK-treated only (*FK*), FK and DNA plasmid only treated (*FK+Plac1-hIGF1*), FK and nanoparticle treated (*FK+NP-Plac1-hIGF1*) and harvested 96 hours after treatment.

Human primary cytotrophoblasts were isolated using a modified method of [12]. Briefly, placental tissue was collected, and villous portion washed and dissected to remove vasculature and connective tissue. The dissected tissue was digested using Trypsin digestion and cell types separated using a 5–70 % Percoll® gradient. The resulting cytotrophoblasts were incubated in cytotrophoblast media (50% DMEM/50% HAM’s F12, 10% FBS, 1% penicillin/streptomycin) for 48 h prior to treatment with nanoparticle to allow for spontaneous differentiation into syncytiotrophoblasts. The resulting syncytiotrophoblasts were then either not treated (*Control*), treated with DNA plasmid only (*Plac1-hIGF1*), or treated with nanoparticle (*NP-Plac1-hIGF1*) and harvested 96 h after treatment.

### RNA Isolation, Reverse Transcription and Quantitative PCR (qPCR)

Following treatment, BeWo and syncytiotrophoblast cells were lysed using RLT Buffer from Qiagen supplemented with 1%  $\beta$ -mercaptoethanol. Total cellular RNA was isolated using the RNeasy mini RNA Isolation kit (*Qiagen*) as per manufacturer’s protocol. RNA quantification was assessed using Nanodrop® Spectrophotometer (*Thermo Fisher*).

1  $\mu\text{g}$  of total RNA was used to generate cDNA using the High Capacity cDNA Reverse Transcription kit following manufacturer’s protocol (*Applied Biosystems*). Oligonucleotide primers for *hIGF1* and housekeeping gene  $\beta$ -actin (*ACTB*) were designed as previously

described [8]. Quantitative PCR was performed using the Power SYBR Green Master Mix (BeWo and syncytiotrophoblast cells; *Applied Biosystems*) or Express SYBR qPCR Supermix (*Invitrogen*) following manufacturers protocol in the Applied Biosystems StepOne-Plus Real-Time PCR System. Relative mRNA expression was calculated using the StepOne Software v2.3 (*Applied Biosystems*) by the comparative CT method [13].

### **In vitro human placenta fragment culture, in situ hybridization and immunohistochemistry**

Term human placentas were collected and villous fragment samples dissected to a size of approximately 5 mm, washed free of maternal blood with PBS and cultured in cytotrophoblast media for 120 h prior to nanoparticle treatment in order to allow for syncytiotrophoblast layer regeneration [14]. At 120 h, fragments were treated with the either the nanoparticle containing a plasmid encoding the Green Fluorescent Protein (*NP-GFP*) gene as a control treatment or nanoparticle containing a plasmid encoding the *hIGF1* gene (*NP-Plac1-hIGF1*) and snap frozen or fixed and paraffin embedded at 24, 48, and 72 h after treatment. Fragment viability was assessed at 48 h in untreated and NP-Plac1-hIGF1 treated fragments by measuring lactate dehydrogenase (LDH) release using the Pierce LDH Cytotoxicity Assay Kit (*Thermo Scientific*) follow manufacturer's instructions.

To quantify *hIGF1* and nutrient transporter mRNA expression using qPCR, RNA was collected by homogenizing in Trizol (*Invitrogen*) and extracting using the RNeasy Mini columns as per manufacturers protocol. cDNA was generated and qPCR performed as previously described [8]. Primer sequences were as follows: *hIGF1 F*:

TTTTGTGATTTCTTGAAGGTGA, *R*: CGGTCCAGCCGTGGCAGA; *SLC2A1 F*:  
 CCCC AATTTTGGCTCCAAGG, *R*: CCAGAATGACACGGATGCTC; *SLC38A1 F*:  
 GCAGTGGGATTTTGGGACTC, *R*: ACAGCAATGTC ACTGAAGTCAA; *SLC38A2 F*:  
 CCTTTGTGATCCAGGCATT, *R*: CCAATGACACCAACAGAACCA; *TBP F*:  
 GAACCACGGCACTGATTTTC, *R*: TGCCAGTCTGGACTGTTCTTC;  $\beta$ -*ACTIN F*:  
 CGCGAGAAGATGACCCAG, *R*: TAGCACAGCCTGGATAGCAA.

In situ hybridization to determine plasmid specific mRNA expression in term human fragments was performed using a custom designed BaseScope™ probe (*Advanced Cell Diagnostics*) specific to the sequence between the stop codon and the polyA signal of the plasmid. 5 µm PFA-fixed, paraffin embedded tissue sections were deparaffinised and rehydrated following standard protocols. Extended antigen retrieval was performed by immersing slides in boiling RNAscope™ Targeted Retrieval Reagent (*Advanced Cell Diagnostics*) for 30 min followed by a 30 min RNAscope™ Protease IV (*Advanced Cell Diagnostics*) incubation at 40°C. In situ hybridisation with the BaseScope™ Assay then occurred following manufacturers protocol. Sections were counterstained using haematoxylin and imaged using the Nikon Eclipse 80i microscope

For immunohistochemical analysis of SLC2A1 protein, 3 µm sections were obtained, deparaffinised and rehydrated following standard protocols. Antigen retrieval was performed by boiling sections in target antigen retrieval solution (*Dako*) for 30 mins endogenous peroxidase activity was suppressed by incubating the slides in 3% hydrogen peroxide. The SLC2A1 antibody (*Abcam: ab15309*) was diluted 1:750 in 5% goat serum and 1% bovine serum albumin (BSA) in PBS and applied overnight at 4°C under humidified conditions.

Negative controls were included by omitting the primary antibody from the diluent. SLC2A1 antibody binding was amplified with the Alexafluore 647 goat anti-rabbit (4 µg/mL, *Invitrogen: A21246*) secondary, nuclei counterstained with DAPI and then visualised using the Nikon Eclipse 80i fluorescent microscope.

### Oxidative stress induction and cellular response in BeWo cells

1×10<sup>5</sup> BeWo cells/well were seeded in a 6 well plate and allowed to adhere for 4 hours before being treated nanoparticle (8 µg: *NP-Plac1-hIGF1*) for 24 h. Oxidative stress was then induced by treating the cells with 400 µM of hydrogen peroxide (H<sub>2</sub>O<sub>2</sub>) for 24 h. Live/dead cell counts were performed by collecting cells, staining with trypan blue and counting using a haemocytometer. Cell number was also determined using crystal violet (CV) assay whereby media was aspirated, and cells washed with PBS. A 2% CV in 2% ethanol solution was added and incubated for 20 mins at room temperature. Wells were then washed in running tap water and dried for 2 h before addition of 1% SDS solution. Optical density was measured in triplicate at 570 nm on a micro-titer plate reader (Synergy H1 Hybrid; *Biotek*) and percentage of cells compared to untreated cells. Mitochondrial function was assessed using the Resazurin end point assay where by 300 µL of Resazurin (*Cell Signaling Technologies*) was added to each well containing fresh media and incubated for 2 h at 37°C. The degree of reduction of resazurin was measured by absorbance at 570 nm and 600 nm using a micro-titer plate reader (Synergy H1 Hybrid; *Biotek*). mRNA expression of *hIGF1*, *BAX*, and *BCL2* was determined as previously described with the following primers for *BAX* F: GGACGAACTGGACAGTAACATGG, R: GCAAAGTAGAAAAGGGCGACAAC and *BCL2* F: ATCGCCCTGTGGATGACTGAG, R: CAGCCAGGAGAAATCAAACAGAGG.

### Statistics

All statistical analyses were performed in R (v3.1.1) [15]. Shapiro-Wilke test confirmed normality of the data and all data analyzed using an analysis of Variance (ANOVA) with a post-hoc comparison to calculate exact P-values. For qPCR data, this was a nonparametric ANOVA. For the human placenta fragment experiment, a 2-way ANOVA was used to compare the effect of both nanoparticle treatment and time. Results are reported as mean and standard error of the mean (SEM), or median and interquartile range (IQR) for qPCR data, and statistical significance was deemed at P < 0.05.

## Results

### Human syncytiotrophoblasts are capable of nanoparticle uptake ex vivo

Prior to addition of Texas-red conjugated nanoparticle (NP) to maternal perfusate, no Texas-red fluorescence was recorded in maternal perfusate (Figure 1A). Upon addition of nanoparticle, Texas-red fluorescence increased in maternal perfusate and declined after approximately 1 hour of perfusion (Figure 1A; mean minimum relative fluorescence units (RFU)±SEM: baseline: -1.2±1.3 vs. NP addition: 322.4±62.1 vs. conclusion: 74.9±7.2; P<0.001). No Texas-red fluorescence was detected in the fetal perfusate (Figure 1A: mean minimum RFU±SEM: baseline -0.7±0.6 vs. NP addition 1.5±1.5 vs. conclusion 3.7±2.0; P=0.490). This indicated the nanoparticle did not cross the placental syncytium and was

confirmed through histological analysis of Texas-Red in perfused tissue (Figure 1B; negative control tissue & C; tissue perfused with Texas-red conjugated nanoparticle and 1D; quantification of Texas-red fluorescence in placenta tissue sections).

### **hIGF1 expression is significantly increased in cultured, syncytialized trophoblast cells following treatment with nanoparticle**

FK treatment of BeWo cells induced differentiation (Figure 2A & B) and did not change *hIGF1* expression (Figure 2C). Treatment of differentiated BeWo cells with plasmid alone also did not change *hIGF1* expression. However, treatment with *NP-PLAC1-hIGF1* for 48 h resulted in a 55,000-fold increase in mRNA expression of *hIGF1* when compared to control (Figure 2C;  $P=0.0003$ ). In isolated primary human trophoblasts, a 95-fold increase in expression of *hIGF1* mRNA was seen following *NP-PLAC1-hIGF1* treatment when compared to control (Figure 2D;  $P=0.003$ ).

### **Nanoparticle delivery of hIGF1 resulted in translocation of the SLC2A1 glucose transporter to the syncytial apical and basal membranes**

Treatment of human placenta fragments with *NP-PLAC1-hIGF1* resulted in an 875-fold increase in *hIGF1* expression within 24 h and was sustained until 72 h post-treatment when compared to both control fragments and those treated with *NP-GFP* (Figure 3A;  $P<0.001$ ). In-situ hybridization confirmed plasmid specific mRNA expression in the syncytiotrophoblast cells of tissue 72 h after treatment with nanoparticle (Figure 3B). Functionally, nanoparticle treatment at 48 h did not change LDH release when compared to untreated (LDH release mean  $\pm$  SEM; control:  $0.13 \pm 0.012$  vs. *hIGF1*:  $0.12 \pm 0.016$ ;  $P=0.622$ ). Increased *hIGF1* expression in the syncytiotrophoblasts also did not change mRNA expression of *SLC2A1* (Supplementary Table 1). However, immunohistochemical characterization at 48 h showed translocation from the cytoplasm to the basal and apical membranes of the syncytiotrophoblasts and cytotrophoblast cells indicating a response supportive towards glucose transport (Figure 3C). *SLC38A1* and *SLC38A2* expression at 24 h and 48 h also showed no change in response to nanoparticle treatment (Supplementary Table 1).

### **Increased hIGF1 expression prevents increased cell death under oxidative stress conditions**

*hIGF1* expression was increased in both the *NP-PLAC1-hIGF1* alone and *NP-PLAC1-hIGF1+H<sub>2</sub>O<sub>2</sub>* compared to control and *H<sub>2</sub>O<sub>2</sub>* alone treated (Figure 4A; 1450-fold and 2500-fold increase, respectively,  $P=0.05$ ). *H<sub>2</sub>O<sub>2</sub>* treatment alone resulted in 41% cell death compared to 19% in the control cells and 13% in the *NP-PLAC1-hIGF1* alone treated (Figure 4B,  $P<0.0001$ ). Prior treatment with the *NP-PLAC1-hIGF1* protected against *H<sub>2</sub>O<sub>2</sub>* induced increased cell death (Figure 4B; 24% in the *NP-PLAC1-hIGF1+H<sub>2</sub>O<sub>2</sub>*). This was not due to changes in cell number as a reduction in cell number was observed in the *H<sub>2</sub>O<sub>2</sub>* alone and *NP-PLAC1-hIGF1+H<sub>2</sub>O<sub>2</sub>* treated cells (Figure 4C, control: 100% vs. *NP-PLAC1-hIGF1*: 106% vs. *H<sub>2</sub>O<sub>2</sub>*: 69% vs. *NP-PLAC1-hIGF1 + H<sub>2</sub>O<sub>2</sub>*: 60%,  $P<0.0001$ ) and likely due to detachment of cells from the plate. *BAX:BCL2* mRNA ratio was also not different between any of the treatment groups (Figure 4D,  $P=0.07$ ), nor was there a difference in total antioxidant expression in any of the treatments (Total Antioxidant Capacity mean  $\pm$  SEM;

control:  $47.6 \pm 4.1$ , *NP-PLAC1-hIGF1*:  $49.7 \pm 4.7$ ,  $H_2O_2$ :  $39.5 \pm 6.7$ , *NPPLAC1-hIGF1+H<sub>2</sub>O<sub>2</sub>*:  $47.1 \pm 8.3$ ,  $P=0.52$ ). Analysis of mitochondrial activity, showed a reduction in % rezaurin reduction in the  $H_2O_2$  alone treated cells that *NP-PLAC1-hIGF1* treatment protected against (Figure 4E,  $P=0.003$ ).

## Discussion

Currently, no therapy exists for treating placental insufficiency in cases of spontaneous FGR in humans. We have previously shown that overexpression of *hIGF1* in a mouse model of placental insufficiency can maintain fetal growth [8]. However, human and mouse placentas differ considerably in structure and function and the response of the human placenta to nanoparticle treatment may differ. Consistent advances in the development of nanomedicines has increased interest in understanding how the placenta responds to nanoparticles [16–19]. Whilst some nanoparticles have been shown to cross the placental barrier [20], we are the first to report uptake of a polymer-based nanoparticle for gene therapy into the placental syncytial barrier in an *ex vivo* perfusion model and several different *in vitro* models. Treatment of differentiated BeWo cells, fused primary human trophoblasts, and term placenta fragments resulted in a robust increased expression of the target gene: *hIGF1*, and was significantly higher than that achieved using plasmid alone. Furthermore, we showed the benefits of increased *hIGF1* expression including the translocation of *SLC2A1* within the syncytium that would suggest increased glucose transport and protecting against increased cell death under conditions of oxidative stress. Altogether, these results highlight the potential of this novel therapeutic approach in treating FGR and other placenta-related pregnancy complications.

How effective nanomedicine is in obstetric diseases in the context of placental manipulation not only depends the efficiency of cargo delivery to the placenta but also on the transgene chosen. Impaired nutrient supply to the fetus is one of the leading causes of FGR [21, 22]. We chose *IGF1* because of its ability to improve nutrient transfer to the growing fetus by enhancing placental nutrient transport [9, 23]. In BeWo cells, adenoviral-mediated increased *IGF1* expression increases mRNA expression of *SLC38A1* and *SLC38A2* [9] indicating the ability to enhance amino acid transport. This is also similar for glucose transport in mice placentas [23]. As a result, fetal growth increases, however, this is in the absence of increasing placental weight [24]. In this study, mRNA expression of *SLC38A1* and *SLC38A2* in placenta fragments did not change with nanoparticle treatment or increased *hIGF1* expression. However, it is possible that the time frame in which the fragments were collected was not long enough to increase IGF1 protein expression to a level required to result in changes to mRNA of these nutrient transporters. IGF1 is a secreted protein and current detection methods for measuring IGF1 were not sensitive enough to detect measurable levels in our studies. *In situ* hybridization confirmed plasmid-specific mRNA expression of *hIGF1* in syncytiotrophoblast cells and treatment with the *hIGF1* nanoparticle resulted in translocation of the glucose transporter, *SLC2A1*, to the apical and basal membranes of the syncytiotrophoblasts and cytotrophoblasts. This translocation could be due to IGF1 signaling through mTOR which has previously been shown to mediate trophoblast cell surface expression of System A and System L amino acid transporter activity [25] and in this instance would increase the placental capacity to transfer glucose



from maternal circulation to the fetus which would be beneficial to fetal growth and may be key in treating FGR *in utero*.

Increased placental oxidative stress has also been implicated as a leading cause of placental dysfunction, particularly in the syncytiotrophoblast cells [26, 27]. Building upon prior knowledge that increased *hIGF1* expression increases BeWo cell proliferation and reduces apoptosis [8], here we demonstrate that prior treatment of BeWo cells with our nanoparticle is protective against increased cell death caused by oxidative stress. This was not due to changes in cell number nor in the mRNA expression of the pro-apoptotic gene *BAX* or anti-apoptotic gene *BCL2*. IGF1 receptor binding has been shown to signal through BAX/BCL2 and protect against apoptosis in both mesangial cells and brown preadipocyte cell lines [28, 29] and it is possible that a similar response may occur in our model however, translational changes in *BAX* and *BCL2* need to be further clarified. Increased *hIGF1* expression did however maintain mitochondrial cell activity. Oxidative stress occurs when there is an imbalance between the level of reactive oxygen species (ROS) produced and production of antioxidant defenses. The mitochondrial respiratory chain, which is integral to cellular metabolism, is a major generator of intracellular ROS and as such, mitochondria contain numerous defense mechanisms to detoxify and repair ROS-induced damage [30]. Thus, it is plausible that increased *hIGF1* may be regulating mitochondrial activity, resulting in protection against increased oxidative stress, this phenomenon worth further investigation.

Safety and specificity are two of the biggest barriers in the implementation of nanoparticle-based gene therapies to clinical translation [31]. The present study provides insight into the uptake of our polymer-based nanoparticle into the human placental syncytium both *in vitro* and *ex vivo* which is crucial to developing this technology further. Targeting the placenta; a transient organ no longer required after birth, reduces concerns about long-term effects. Furthermore, using a non-viral polymer, which can be modified to increase target organ specificity, are positive elements for this potential therapeutic. However, whilst we were able to show uptake of the nanoparticle in the *ex vivo* perfusion model, time limitations prevented being able to assess transgene expression in this model. Future experiments have been planned to perform longer (up to 48h [32]) perfusions in order to not only assess transgene expression but to fully determine whether nanoparticle is transferred into the fetal circulation. Another limitation with the current study is the gestational age of the placenta tissue used. Translationally, this form of therapy will most likely be implemented after FGR is diagnosed based on fetal growth trajectory. This usually occurs around 28 weeks gestation. Therefore, the response of placental syncytium during this point of gestation needs to be assessed in conjunction with studies using tissue from term however, the current study provides a strong rationale for undertaking such experiments.

To conclude, we have shown that our polymer-based nanoparticle is able to enter the human placental syncytium resulting in effective delivery of the plasmid and robust increase in cell-specific transgene expression of *hIGF1*. We have also characterized several functional responses to increased *hIGF1* expression including changes in nutrient transporter localization and protection against oxidative stress. Enhancing placental nutrient transfer to the fetus as well as reducing cellular damage caused by oxidative stress may aid in

improving pregnancy outcomes such as iatrogenic preterm birth due to FGR or the associated neonatal morbidities and mortality.

## Supplementary Material

Refer to Web version on PubMed Central for supplementary material.

## Acknowledgements:

We would like to thank Jennifer Courtney at Cincinnati Children's Hospital for their assistance in the ex vivo placenta perfusion experiments, Prof. Craig Duvall and Dr. Mukesh Gupta at Vanderbilt University for producing the HPMA-DMAEMA polymer, and Dr. Dale McAninch at the University of Adelaide for his assistance in the design of the in situ hybridization experiment. Special thanks to the TTUHSC Clinical Research Institute, and the staff and patients at the University of Cincinnati Hospital Labor and Delivery Unit for help with human placenta collections.

This study was funded by Eunice Kennedy Shriver National Institute of Child Health and Human Development (NICHD) awards R01HD068504 and R01HD090657 (HNJ). Placental perfusion system was supported in part by National Institute of Health grant 1R43HD095348-01SUB (NS-L).

## REFERENCES

- [1]. Roberts CT, IFPA Award in Placentology Lecture: Complicated interactions between genes and the environment in placentation, pregnancy outcome and long term health, *Placenta* 31 Suppl (2010) S47–53. [PubMed: 20096927]
- [2]. Burton GJ, Fowden AL, The placenta: a multifaceted, transient organ, *Philosophical transactions of the Royal Society of London. Series B, Biological sciences* 370(1663) (2015) 20140066. [PubMed: 25602070]
- [3]. Enders AC, Blankenship TN, Comparative placental structure, *Advanced drug delivery reviews* 38(1) (1999) 3–15. [PubMed: 10837743]
- [4]. Fowden AL, The insulin-like growth factors and feto-placental growth, *Placenta* 24(8–9) (2003) 803–12. [PubMed: 13129676]
- [5]. Powell-Braxton L, Hollingshead P, Warburton C, Dowd M, Pitts-Meek S, Dalton D, Gillett N, Stewart TA, IGF-I is required for normal embryonic growth in mice, *Genes Dev* 7(12B) (1993) 2609–17. [PubMed: 8276243]
- [6]. Giudice LC, van Dessel HJ, Cataldo NA, Chandrasekher YA, Yap OW, Fauser BC, Circulating and ovarian IGF binding proteins: potential roles in normo-ovulatory cycles and in polycystic ovarian syndrome, *Prog Growth Factor Res* 6(2–4) (1995) 397–408. [PubMed: 8817683]
- [7]. Nieto-Diaz A, Villar J, Matorras-Weinig R, Valenzuela-Ruiz P, Intrauterine growth retardation at term: association between anthropometric and endocrine parameters, *Acta Obstet Gynecol Scand* 75(2) (1996) 127–31. [PubMed: 8604597]
- [8]. Abd Ellah N, Taylor L, Troja W, Owens K, Ayres N, Pauletti G, Jones H, Development of Non-Viral, Trophoblast-Specific Gene Delivery for Placental Therapy, *PloS one* 10(10) (2015) e0140879. [PubMed: 26473479]
- [9]. Jones H, Crombleholme T, Habli M, Regulation of amino acid transporters by adenoviral-mediated human insulin-like growth factor-1 in a mouse model of placental insufficiency in vivo and the human trophoblast line BeWo in vitro, *Placenta* 35(2) (2014) 132–8. [PubMed: 24360522]
- [10]. Carrillo M, Chuecos M, Gandhi K, Bednov A, Moore DL, Maher J, Ventolini G, Ji G, Schlabritz-Loutsevitch N, Optical tissue clearing in combination with perfusion and immunofluorescence for placental vascular imaging, *Medicine* 97(39) (2018) e12392. [PubMed: 30278515]
- [11]. Jain A, Schneider H, Aliyev E, Soydemir F, Baumann M, Surbek D, Hediger M, Brownbill P, Albrecht C, Hypoxic treatment of human dual placental perfusion induces a preeclampsia-like inflammatory response, *Lab Invest* 94(8) (2014) 873–80. [PubMed: 24933425]
- [12]. Kliman HJ, Feinberg RF, Haimowitz JE, Human trophoblast-endometrial interactions in an in vitro suspension culture system, *Placenta* 11(4) (1990) 349–67. [PubMed: 2235916]

- [13]. Pfaffl MW, A new mathematical model for relative quantification in real-time RT-PCR, *Nucleic Acids Res* 29(9) (2001) e45. [PubMed: 11328886]
- [14]. Siman CM, Sibley CP, Jones CJ, Turner MA, Greenwood SL, The functional regeneration of syncytiotrophoblast in cultured explants of term placenta, *American journal of physiology. Regulatory, integrative and comparative physiology* 280(4) (2001) R1116–22.
- [15]. R.D.C. Team, R: A Language and Environment for Statistical Computing, R Foundation for Statistical Computing, Vienna, Austria, 2011.
- [16]. Chu M, Wu Q, Yang H, Yuan R, Hou S, Yang Y, Zou Y, Xu S, Xu K, Ji A, Sheng L, Transfer of quantum dots from pregnant mice to pups across the placental barrier, *Small* 6(5) (2010) 670–8. [PubMed: 20143348]
- [17]. Grafmueller S, Manser P, Diener L, Diener PA, Maeder-Althaus X, Maurizi L, Jochum W, Krug HF, Buerki-Thurnherr T, von Mandach U, Wick P, Bidirectional Transfer Study of Polystyrene Nanoparticles across the Placental Barrier in an ex Vivo Human Placental Perfusion Model, *Environmental health perspectives* 123(12) (2015) 1280–6. [PubMed: 25956008]
- [18]. Semmler-Behnke M, Kreyling WG, Lipka J, Fertsch S, Wenk A, Takenaka S, Schmid G, Brandau W, Biodistribution of 1.4- and 18-nm gold particles in rats, *Small* 4(12) (2008) 2108–11. [PubMed: 19031432]
- [19]. Yamashita K, Yoshioka Y, Higashisaka K, Mimura K, Morishita Y, Nozaki M, Yoshida T, Ogura T, Nabeshi H, Nagano K, Abe Y, Kamada H, Monobe Y, Imazawa T, Aoshima H, Shishido K, Kawai Y, Mayumi T, Tsunoda S, Itoh N, Yoshikawa T, Yanagihara I, Saito S, Tsutsumi Y, Silica and titanium dioxide nanoparticles cause pregnancy complications in mice, *Nature nanotechnology* 6(5) (2011) 321–8.
- [20]. Saunders M, Transplacental transport of nanomaterials, *Wiley interdisciplinary reviews. Nanomedicine and nanobiotechnology* 1(6) (2009) 671–84. [PubMed: 20049824]
- [21]. Cetin I, Radaelli T, Taricco E, Giovannini N, Alvino G, Pardi G, The endocrine and metabolic profile of the growth-retarded fetus, *Journal of pediatric endocrinology & metabolism : JPEM* 14 Suppl 6 (2001) 1497–505. [PubMed: 11837506]
- [22]. Economides DL, Nicolaidis KH, Blood glucose and oxygen tension levels in small-for-gestational-age fetuses, *American journal of obstetrics and gynecology* 160(2) (1989) 385–9. [PubMed: 2916623]
- [23]. Jones HN, Crombleholme T, Habli M, Adenoviral-mediated placental gene transfer of IGF-1 corrects placental insufficiency via enhanced placental glucose transport mechanisms, *PloS one* 8(9) (2013) e74632. [PubMed: 24019972]
- [24]. Gluckman P, Harding J, The regulation of fetal growth, in: Hernandez M, Argente J (Eds.), *Human growth: basic and clinical aspects*, Elsevier, Huntington, NY, 1992, pp. 253–259.
- [25]. Rosario FJ, Kanai Y, Powell TL, Jansson T, Mammalian target of rapamycin signalling modulates amino acid uptake by regulating transporter cell surface abundance in primary human trophoblast cells, *J Physiol* 591(3) (2013) 609–25. [PubMed: 23165769]
- [26]. Redman CW, Sargent IL, Staff AC, IFPA Senior Award Lecture: making sense of pre-eclampsia - two placental causes of preeclampsia?, *Placenta* 35 Suppl (2014) S20–5. [PubMed: 24477207]
- [27]. Jauniaux E, Poston L, Burton GJ, Placental-related diseases of pregnancy: Involvement of oxidative stress and implications in human evolution, *Human reproduction update* 12(6) (2006) 747–55. [PubMed: 16682385]
- [28]. Boucher J, Macotela Y, Bezy O, Mori MA, Kriauciunas K, Kahn CR, A kinase-independent role for unoccupied insulin and IGF-1 receptors in the control of apoptosis, *Science signaling* 3(151) (2010) ra87. [PubMed: 21139139]
- [29]. Kang BP, Urbonas A, Baddoo A, Baskin S, Malhotra A, Meggs LG, IGF-1 inhibits the mitochondrial apoptosis program in mesangial cells exposed to high glucose, *American journal of physiology. Renal physiology* 285(5) (2003) F1013–24. [PubMed: 12876069]
- [30]. Ott M, Gogvadze V, Orrenius S, Zhivotovsky B, Mitochondria, oxidative stress and cell death, *Apoptosis : an international journal on programmed cell death* 12(5) (2007) 913–22. [PubMed: 17453160]

- [31]. Wong JKL, Mohseni R, Hamidieh AA, MacLaren RE, Habib N, Seifalian AM, Limitations in Clinical Translation of Nanoparticle-Based Gene Therapy, *Trends Biotechnol* 35(12) (2017) 1124–1125. [PubMed: 28822599]
- [32]. Polliotti BM, Holmes R, Cornish JD, Hulsey M, Keesling S, Schwartz D, Abramowsky CR, Huddleston J, Panigel M, Nahmias AJ, Long-term dual perfusion of isolated human placental lobules with improved oxygenation for infectious diseases research, *Placenta* 17(1) (1996) 57–68. [PubMed: 8710814]

### Highlights

- Nanoparticle uptake in human placenta syncytium was determined in an *ex vivo* and several *in vitro* models
- Nanoparticle treatment increased *human insulin-like 1 growth factor (hIGF1)* transgene expression
- Increased *hIGF1* causes translocalisation of glucose transport 1 in syncytiotrophoblast cells
- Increased *hIGF1* protects against increased cell death and decreased mitochondrial activity

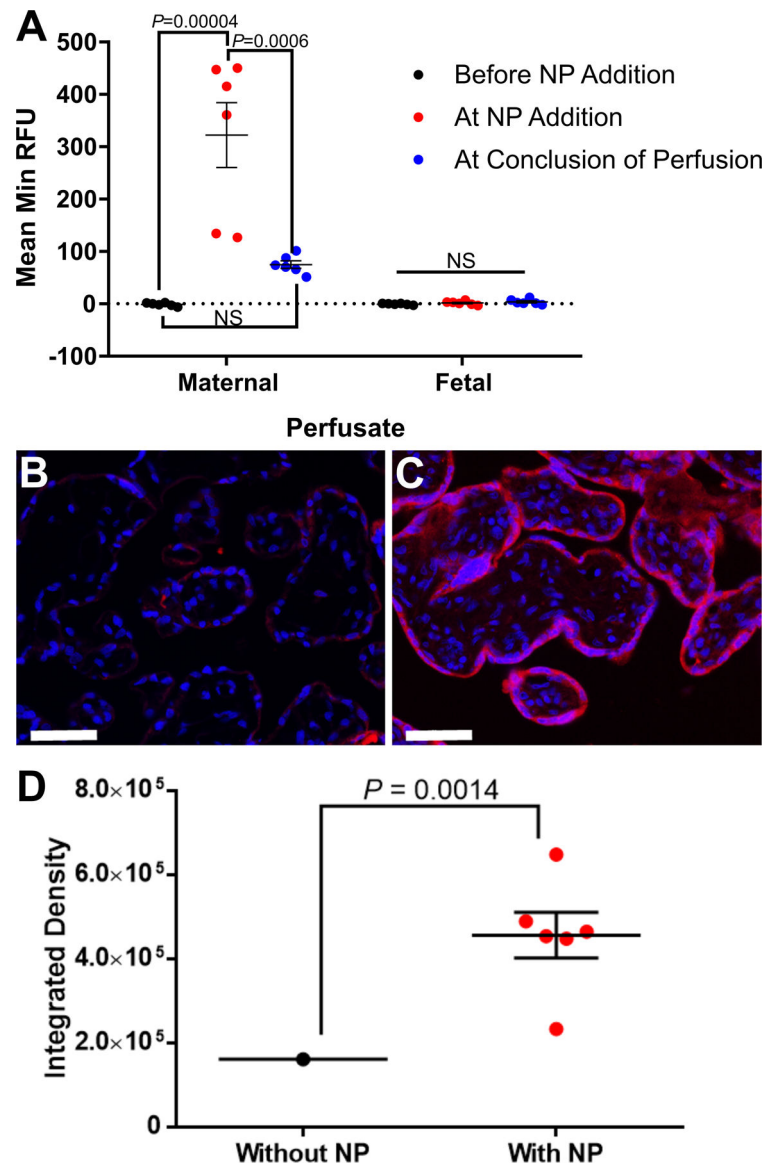


**Figure 1. Analysis of Texas-red fluorescence in maternal and fetal perfusate samples, and placental tissue from the dual placental perfusion experiments.** Prior to addition of Texas-red conjugated nanoparticle (NP) to maternal perfusate, no Texas-red fluorescence was recorded in maternal perfusate (A). Upon addition of nanoparticle, Texas-red fluorescence increased in maternal perfusate and declined after approximately 1 hour of perfusion. Texas-red fluorescence was not determined in fetal perfusate at any of the time points (A). Histological analysis of placental tissue collected at the conclusion of the experiment showed nanoparticle localization in the syncytiotrophoblast layer of the fetal villi (B negative control tissue: perfused tissue with no Texas-red conjugated nanoparticle added, C positive tissue: tissue perfused with Texas-red conjugated nanoparticle for approximately 1 hour). Fluorescence analysis of the tissue sections confirmed a significant increase in Texas-red in the tissue sections exposed to nanoparticle (D). Data are mean  $\pm$  SEM, n=7 term placentas perfused; n=6 term placentas perfused with NP. Statistical significance

determined with an ANOVA and Tukey's post hoc analysis (**A**) and Mann-Whitney test (**D**).  
Scale bar = 50  $\mu$ m.

Author Manuscript

Author Manuscript

Author Manuscript

Author Manuscript

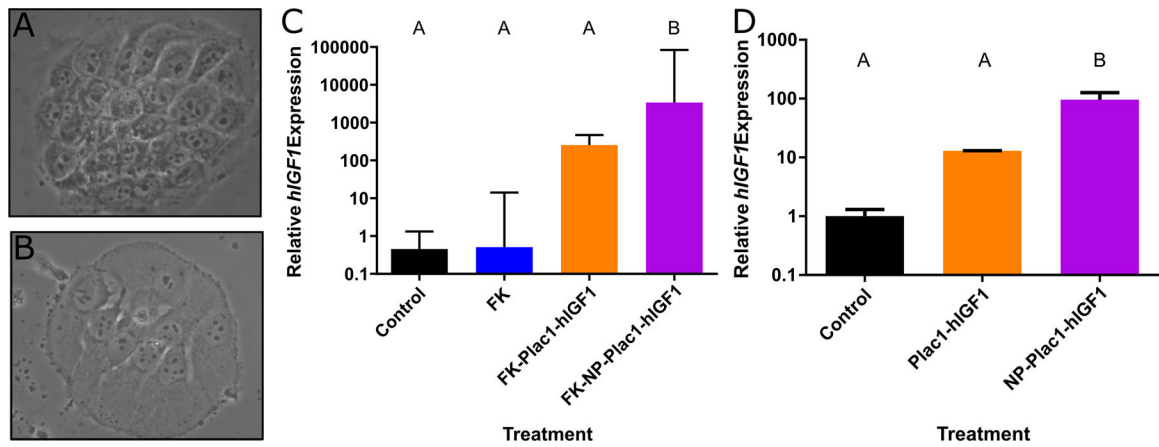


**Figure 2. qPCR analysis of human insulin-like growth factors 1 (hIGF1) mRNA expression in differentiated BeWo and isolated human placental syncytiotrophoblasts after nanoparticle treatment.**

Forskolin treatment of BeWo cells for 24 hours induced differentiation and formation of syncytial-like cells (A and B). qPCR analysis of hIGF1 expression in differentiated BeWo cells showed no difference in mRNA expression in untreated (control), forskolin treated (FK), nor forskolin + plasmid alone treated (FK+Plac1-hIGF1) cells, however, a significant increase in hIGF1 mRNA expression was found in the forskolin + hIGF1 nanoparticle (FK +NP-Plac1-hIGF1) treated cells (C). Similarly in isolated syncytiotrophoblast cells, treatment with plasmid alone (Plac1-hIGF1) did not increase hIGF1 mRNA expression compared to untreated (control) but nanoparticle (NP-Plac1-hIGF1) treatment resulted in a significant increase (D). Data are median  $\pm$  interquartile range, n=6 passages (C) and n=4 isolated placentas (D). Statistical significance was determined with a Kruskal-Wallis test and Dunn's post hoc analysis.



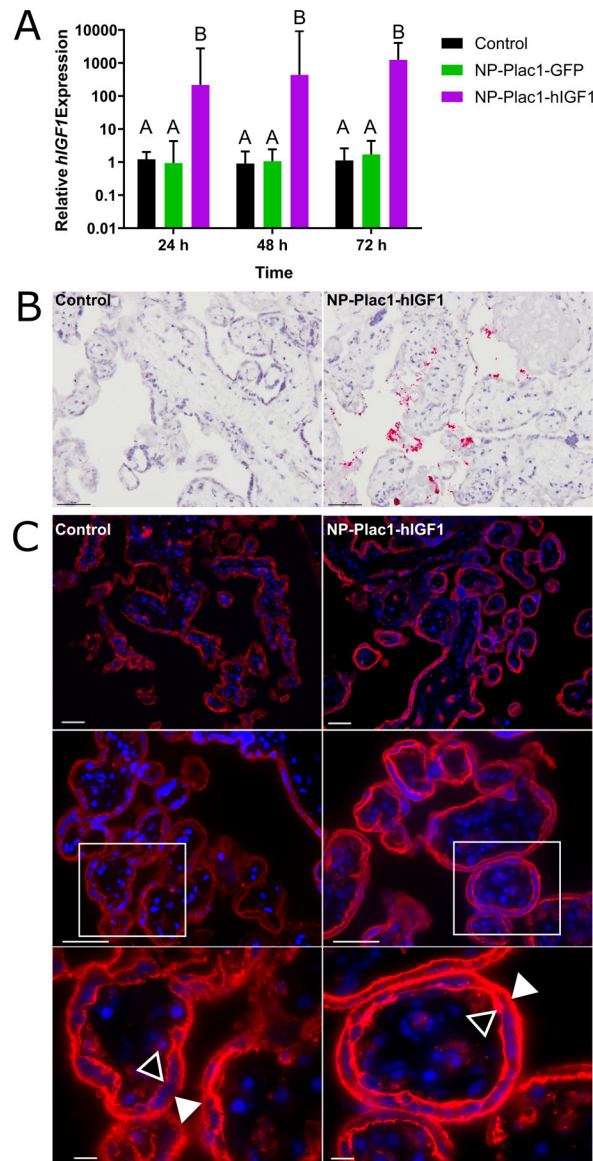


**Figure 3. qPCR analysis of human insulin-like 1 (hIGF1) mRNA expression and immunohistochemical (IHC) localization of glucose transporter 1 (SLC2A1) in placenta fragments treated with nanoparticle.**

qPCR analysis of hIGF1 mRNA showed a significant increase in placenta fragments treated with nanoparticle (NP-Plac1-hIGF1) at 24 hours which was sustained at 72 hours (A). There was no increase in hIGF1 mRNA expression in fragments treated with nanoparticle containing a plasmid encoding the green fluorescent protein gene (NP-Plac1-GFP)(A). In situ hybridization confirmed plasmid specific mRNA expression of IGF1 in syncytiotrophoblast cells of fragments 72 h after treatment with NP-Plac1-hIGF1 and not in untreated fragments (B). Representative images of IHC staining of SLC2A1 in fragments at 48 hours showed trans-localization of the transporter to the apical (closed triangle) and basal (open triangle) membranes of the syncytiotrophoblast and cytotrophoblasts cells in the fragments treated with nanoparticle (NP-Plac1-hIGF1) compared to untreated (control) (C). Data are median  $\pm$  interquartile range, n=6 term placentas. Scale Bar: 200  $\mu$ m (C top row),

50  $\mu\text{m}$  (**B** and **C middle row**), 10  $\mu\text{m}$  (**C bottom row**). Statistical significance was determined with a 2-way ANOVA.

Author Manuscript

Author Manuscript

Author Manuscript

Author Manuscript

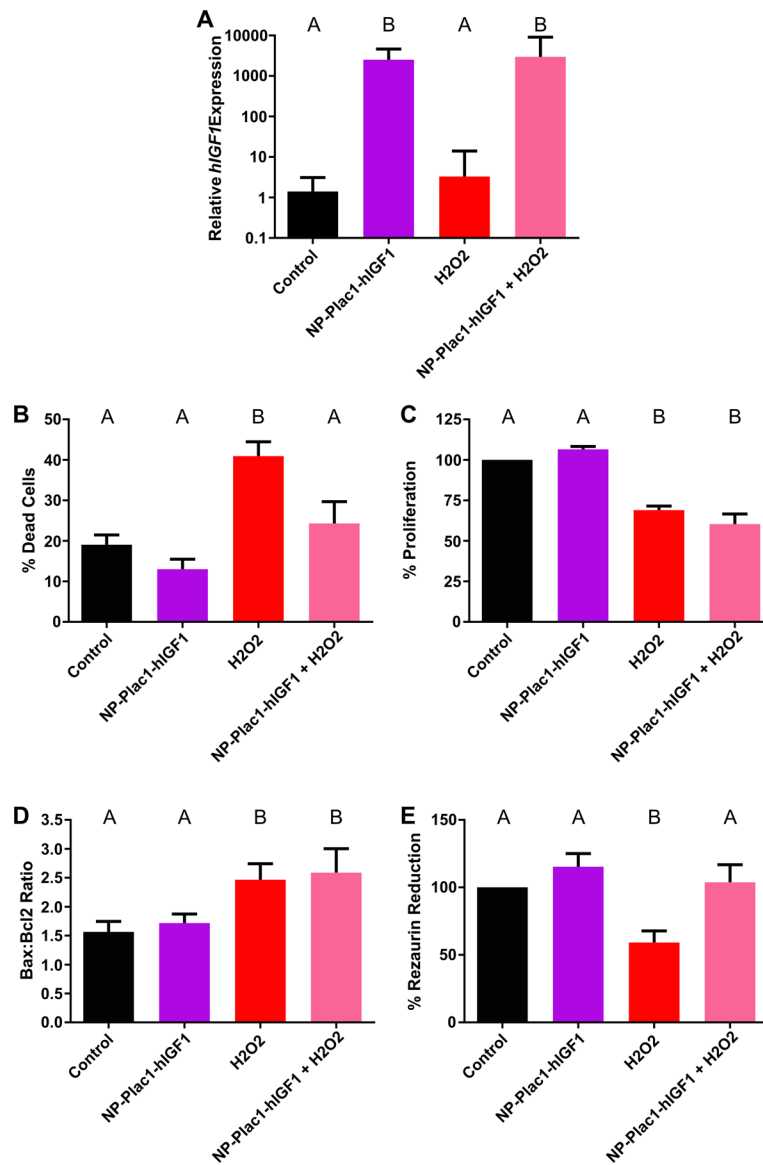


**Figure 4. Functional effect of nanoparticle treatment in protecting against oxidative stress in BeWo cells.**

qPCR analysis of human insulin-like growth factor 1 (hIGF1) was increased in cells treated with nanoparticle (NP-Plac1-hIGF1 and H<sub>2</sub>O<sub>2</sub>+NP-Plac1-hIGF1) compared to untreated (control) and H<sub>2</sub>O<sub>2</sub> alone (A). Compared to untreated, treatment with H<sub>2</sub>O<sub>2</sub> significantly increased the percentage of dead cells but not when cells were pretreated with nanoparticle (B). Cell number was lower in cells treated with H<sub>2</sub>O<sub>2</sub> alone and nanoparticle with H<sub>2</sub>O<sub>2</sub> compared to untreated and nanoparticle alone treated (C). The BAX:BCL2 ratio was higher in cells treated with H<sub>2</sub>O<sub>2</sub> as well as in those treated with nanoparticle and H<sub>2</sub>O<sub>2</sub> when compared to untreated and nanoparticle alone treated (D). Mitochondrial activity, as measured by the percentage of resazurin reduction, was lower in cells treated with H<sub>2</sub>O<sub>2</sub> alone compared to untreated but not in cells treated with nanoparticle prior to H<sub>2</sub>O<sub>2</sub> treatment (E). Data are median ± interquartile range (A) or mean ± SEM (B-E), n=6

passages. Statistical significance was determined with a repeated measures ANOVA and Sidak's multiple comparison test.

Author Manuscript

Author Manuscript

Author Manuscript

Author Manuscript